IEEE Access
Multidisciplinary | Rapid Review | Open Access Journal

Received January 23, 2021, accepted March 2, 2021, date of publication March 17, 2021, date of current version March 26, 2021.

Digital Object Identifier 10.1109/ACCESS.2021.3066192

Analysis of Effect of Motion Path on Leg Muscle Load and Evaluation of Device to Support Leg Motion During Robot Operation by Reducing Muscle Load

HIROKI KATO, TATSURO TERAKAWA, MASAHARU KOMORI, (Member, IEEE), AND IKKO YASUDA

Department of Mechanical Engineering and Science, Kyoto University, Kyoto 615-8540, Japan

Corresponding author: Tatsuro Terakawa (terakawa@me.kyoto-u.ac.jp)

This work was supported by the JSPS KAKENHI Grant Number 19H02053.

ABSTRACT Because the human arm and leg have a similar skeletal structure, it may be possible to use the leg to operate a robot by the master-slave method. However, operation by the leg with six degrees of freedom has two problems. First, people move their ankle with a curved motion despite intending to move it linearly. Second, it is a burden for the operator to suspend their legs in the air during operation. This study dealt with these problems. For the first problem, we hypothesized that one of the reasons was that the muscle load of a curved motion was smaller than that of a linear motion, and we quantitatively compared them by musculoskeletal analysis. The muscle loads of curved motions were 20% smaller in the anteroposterior direction, 3.1% to 23.8% smaller in the lateral direction, and 10% smaller in the vertical direction than linear motions, which showed that the hypothesis was consistent. Further, comparison of the analysis results with the results of a previous study suggested that subjects unconsciously tried to reduce the muscle load and to move closer to a linear line when they moved their ankle while consciously intending to make a linear motion. For the second problem, we developed two different prototypes of a leg support device. An experiment to evaluate the effectiveness of these devices showed that subjective exercise intensity of the tasks in the experiment using the devices was 40% or more less than that without the device, which proved the effectiveness of the devices.

INDEX TERMS Lower limb, operation, gesture, musculoskeletal analysis, gravity compensation.

I. INTRODUCTION

Robot arms with multiple degrees of freedom (DOFs) are used in factories and welfare fields. One of the methods to operate such a robot is master-slave operation, where an operator moves his or her arm to create the same movement in the robot. In this method, the operator can easily understand the correspondence between the movement of the arm and the movement of the robot, which makes it easy for even an inexperienced person to operate the robot. Therefore, many studies related to this operation method have been reported. For example, systems to operate the robot arm by measuring the movement of the human arm with cameras and sensors have been investigated [1]–[10]. Also, various studies have examined robot arm operation by using an exoskeleton-like device [11]–[14] or by using electromyography [15], [16]. Komori *et al.* proposed a virtual space-based evaluation system to compare the master-slave method with a button operation method and proved the effectiveness of the master-slave method by showing that it can shorten the operation time by 27.7% and increase the subjective operability evaluation by 76.0% during operation of a virtual robot hand [17].

The human lower limb has a skeletal system similar to that of the upper limb. Therefore, it may be possible to command a six-DOF operation in the master-slave system by using the leg like the arm. However, because the lower limbs are usually used for walking, there are many studies on walking,

The associate editor coordinating the review of this manuscript and approving it for publication was Guilin Yang.

but few studies on robotic manipulation with the legs. Several studies dealt with a robot manipulation using four DOFs of a lower limb: forward/backward and left/right foot movements and the dorsiflexion/plantarflexion and the valgus/varus of the ankle [18]–[19]. Komori *et al.* studied robot operation by lower limb movement and experimentally showed that the lower limb is inferior to the upper limb for six-DOF operation in terms of time by approximately 79% and the subjective operability evaluation by approximately 39%, but the operability of the lower limb may be relatively close to that of the upper limb in terms of position operation [20].

On the other hand, multi-DOF robot operation using the lower limb has two problems. One is the difference between the operator's intended leg motion and the actual motion. Komori *et al.* conducted experiments that assumed operation of a device using the leg and clarified that, without visual feedback, the path of the ankle center was curved even when the test subject intended to move the ankle linearly [21]. However, the reason for this behavior is not clear, and it is necessary to reveal the reason to improve the method of operation by lower limb movement. Thus, this study conducted musculoskeletal analysis for three-DOF position manipulation [22], [23] and quantitatively evaluated the muscle load during operation by the lower limbs because the muscle load in the motion is assumed to be related to the abovementioned motion characteristics. Through the analysis, we clarified the specific leg motions that reduced the muscle load and investigated the reason for the observed motion characteristics by comparing them with the previous experimental results [21].

The second problem is the muscle load on the lower limb during movement. In multi-DOF operation by the lower limb, the foot should remain suspended in the air, and it is physically burdensome to maintain this position for a long time. Therefore, a method that reduces the muscle load without interfering with motion of the lower limb is necessary. For the upper limbs, Hasegawa *et al.* developed a wearable support device to compensate for the force of gravity on the upper limb and wrist for patients with muscle weakness [24]. For the lower limbs, Barazesh *et al.* researched a wearable gait support device that reduces metabolic costs, including muscle load, during walking [25]. However, there has been no research on reducing the muscle load of a lower limb suspended in the air for a long time. In this study, we developed devices to reduce this muscle load by supporting the lower limbs with a counterforce as large as the gravity force applied to a lower limb suspended in air. We first propose the concept of the device, then discuss the supporting force theoretically, and finally confirm the effectiveness of the proposed device with prototypes.

II. MUSCULOSKELETAL ANALYSIS OF ANTEROPOSTERIOR, LATERAL, AND VERTICAL LEG MOVEMENT

Komori *et al.* conducted experiments on operation of a device using the leg and found that the ankle path was curved when visual feedback was unavailable, even when the test subjects intended to move the ankle linearly [21]. However, the reason was not clear. One possible factor is the musculoskeletal system of the human body. In this study, we focused on the muscle load and evaluated it quantitatively by musculoskeletal analysis to clarify the advantages with respect to muscle load when a person moves his or her leg along a curved path.

A. PREVIOUS RESULTS ON THE DIFFERENCE BETWEEN INTENDED AND ACTUAL LEG MOTION

We discuss the results of an experiment on the difference between the intended leg motion and the actual leg motion reported in previous research [21]. In that study, the experiment was conducted as master-slave operation in which the position of the end effector of the robot arm tracked the motion of the ankle center. Fig. 1 shows the setup of that experiment. A virtual space was displayed on the monitor, where an imaginary operated object (IOO) moved up/down, left/right, and back/forth. The test subjects were instructed to move their leg so that the ankle moved in the same manner as the IOO, as if they were operating the IOO with their leg. At that time, the movement of the ankle center of 10 test subjects was measured. The movement of the IOO is considered to be the movement of the leg that the test subjects intended. The intended leg motion was compared with the actual leg motion. In the experiment, the test subjects only looked at the monitor and did not see their leg movements.

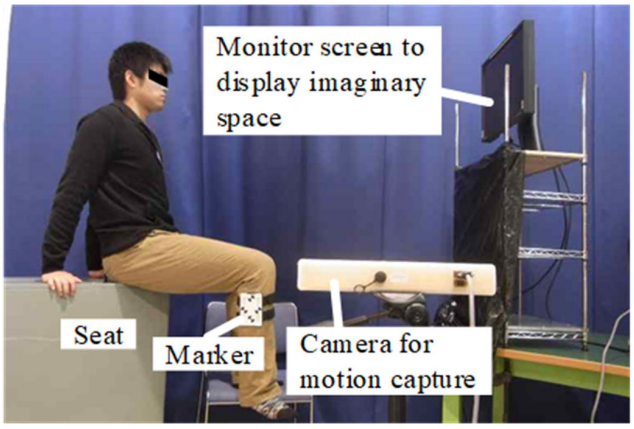

FIGURE 1. Experiment in the previous research. The experiment in which the leg was moved so that the ankle center made the same movement as that shown on the monitor [21].

The experiments clarified that the actual leg motion was curved even when a linear motion was intended. We can explain the cases where the IOO moved linearly in the anteroposterior/lateral direction. Fig. 2(a) shows examples of the path of the measured ankle center when an anteroposterior movement was intended. The ankle center made a curved motion with a convex downward path while moving in an approximately anteroposterior direction. Fig. 3 illustrates this movement schematically, where the test subject intended to perform the linear motion shown by the dashed line, but they actually performed the curved motion shown by the solid

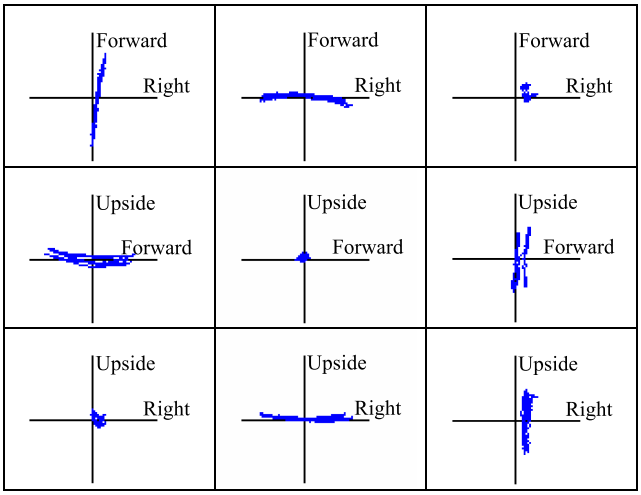

(a) Intending to move in the anteroposterior direction (b) Intending to move in the lateral direction (c) Intending to move in the vertical direction

FIGURE 2. Experimental results of actual trajectory of the ankle center, as obtained in previous research [21].

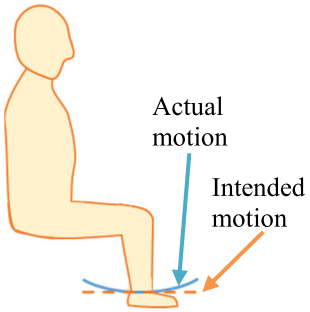

FIGURE 3. Intended and actual anteroposterior motion.

line. The measured path when lateral motion was intended is shown in Fig. 2(b). The path was a curve convexly in the downward and forward directions while moving in an approximately lateral direction. Fig. 4 shows this situation, where the intended movement was linear, but the actual motion was curved. Thus, it was clarified that the characteristic movement of the leg deviates from the intended linear motion and curves despite the intention of an anteroposterior lateral movement. In contrast, in the experimental result for vertical movement shown in Fig. 2(c), the vertical movement was almost linear (only slightly curved), whereas a few test subjects performed curved movements, as shown by the dotted line in Fig. 5.

The reason why such leg movement characteristic occurs was not clarified by Komori and Miyauchi [21]. Thus, this study aims to clarify this reason from the viewpoint of the muscle load on the leg. Our first hypothesis is that a curved motion is caused even when the linear motion is intended in anteroposterior and lateral movements because the muscle load of a curved motion is smaller than that of a linear motion. Also, we formed a second hypothesis that the reason why

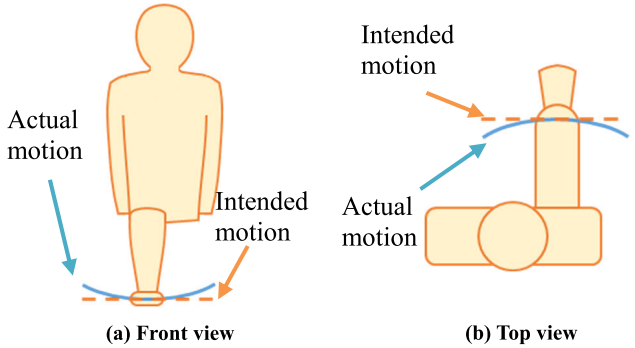

(a) Front view (b) Top view

FIGURE 4. Intended and actual lateral motion.

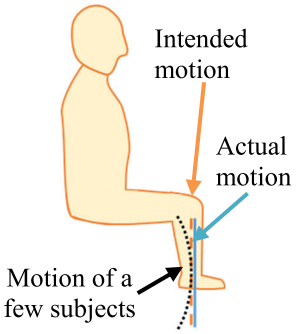

FIGURE 5. Intended and actual vertical motion.

both curved and uncurved motion was observed when a linear motion was intended in the vertical movement is that the difference in the muscle load between the former and the latter is small, but the muscle load of the former is slightly smaller than that of an uncurved motion. To prove the relation of the muscle loads in these hypotheses, we calculated and compared the muscle loads for both linear and curved motions.

B. ANALYSIS METHOD

In this study, we performed an inverse dynamics analysis of leg movements with a human musculoskeletal model. The produced muscle force and the required energy in each muscle were calculated based on the given movement of the leg. We clarified the magnitude of muscle loads caused by various leg movements by analyzing them as linear motions and curved motions. The musculoskeletal model analysis was carried out with the software AnyBody (AnyBody Technology Inc.), which calculates inverse dynamics to obtain joint reaction force, joint moment, muscle force, and muscle activity when the movements and boundary conditions of the musculoskeletal model are input. We describe the calculation method in AnyBody in detail. In the human body, the number of muscles is more than that of the DOFs of joints, which produces a redundant system. Therefore, the inverse dynamics problem, namely, obtaining the input muscle force from the output joint torque and force, is ill-posed. To address this dilemma, the calculation is carried out according to (1) in

AnyBody.

$$\begin{aligned} &\min : \sum_{i=1}^{n} \left(\frac{f_i}{N_i} \right)^3 \\ &\text{subject to} : \mathbf{Cf} = \mathbf{d} \\ &0 < f_i < N_i (i = 1, \ldots, n), \end{aligned} \tag{1}$$

where n is the total number of muscles, f_i is the force produced by muscle i, N_i is the maximum force that muscle i can produce, and f_i/N_i represents the activity of muscle i. The objective problem is the equilibrium equation, where $\mathbf{C}$ is the coefficient matrix, $\mathbf{f}$ is the vector of all unknown forces, and $\mathbf{d}$ is the vector of all known loads. The objective function is the sum of the cube of the muscle activities, and the muscle force to minimize this function is searched. This is based on the assumption that muscles produce forces to minimize the aggregate muscle stress [26].

We use the metabolic energy E_{me} as an index showing the magnitude of muscle load. The value of E_{me} represents the energy necessary for the muscle to produce the force. The smaller the value is, the smaller the muscle load is. Then, E_{me} is suitable for comparing muscle loads between different movements. For example, Zhou *et al.* calculated and compared the value of E_{me} for the trajectory of a hand moving between two points on a plane by using several musculoskeletal models [27]. In the research by Wolf *et al.*, the design of a car trunk was discussed by comparing the values of E_{me} for various parameters in the work of lifting objects into cars [28].

Fig. 6 shows the musculoskeletal model that we used in the analysis. The human model is based on the standard model of AnyBody, which corresponds to an adult 1800 mm tall and weighing 75 kg. The pelvis is fixed in the space, and the upper body is fixed in an upright state. The x-axis of the coordinate system is parallel to the anteroposterior direction, the y-axis is parallel to the vertical direction, and the z-axis is parallel to the lateral direction. The positive direction of each axis is forward, upward, and rightward, respectively. This analysis deals with the right leg, and the left leg and both arms were omitted from the model because they are unrelated to the movement of the right leg.

In this analysis, as shown in Fig. 6, the reference posture is defined as the condition in which the vector from the hip joint to the knee joint is horizontal and faces the same direction as the body, and the ankle joint is positioned directly below the knee joint. This posture is the same as the reference posture before starting leg movement in the study of Komori and Miyauchi [21]. In the musculoskeletal model, the reference posture corresponds to the condition that the angles of the flexion, abduction, and external rotation of the hip joint are 90°, 0°, and −1.8°, respectively, and the knee flexion angle is 91.3°. The external rotation angle of the hip joint is −1.8° and the flexion angle of the knee joint is 91.3° because the angle between the line passing through the centers of the hip and knee joints and the line passing through the centers of the knee and ankle joints is set as 90° on the x-y plane.

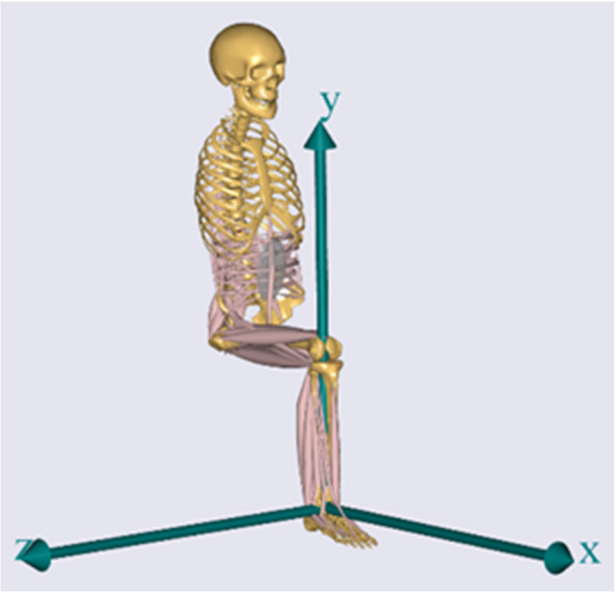

FIGURE 6. Analysis model and spatial fixed coordinate system in the reference posture.

The position of the ankle center in the reference posture is the origin of the coordinate system.

C. ANALYSIS CONDITIONS

This study analyzed the movements of the leg in which the ankle center starts from the reference posture and moves in the anteroposterior, lateral, and vertical directions. This is the same as the motion discussed in the previous study [21]. In addition, we addressed both motions, that is, the linear motion intended by the test subjects and the actual curved motion they produced, as shown in the previous study.

Next, we explain the trajectory of the ankle center used for the analysis for each of the anteroposterior, lateral, and vertical movements. The anteroposterior movement is made mainly in the x-axis direction. In the previous study, the path of the ankle center in the anteroposterior movement was characterized by a curve that was convex in the negative y-axis direction, that is, it was downward. Taking this result into consideration, the trajectory of the ankle center in the analysis is defined by (2) using a quadratic function.

$$\begin{cases} x(t) = \pm L(-1 + 2\displaystyle\int_0^t v(\tau)\, d\tau) \\ y(t) = (a_B/L)x(t)^2 \\ z(t) = 0 \end{cases} \quad (0 \le t \le t_o), \tag{2}$$

where a_B is a constant representing the quadratic coefficient. The range of motion of the ankle center is restricted within the space of a cube 300 mm on each side, and $L = 150$ mm is half of this range of motion. The velocity of the ankle center $v(t)$ and movement time t_0 are described in detail later. The plus–minus sign in $x(t)$ represents the direction of the movement: a plus sign represents forward movement, and a minus sign represents backward movement. The coefficient a_B/L in $y(t)$

is used to make the quadratic coefficient a_B independent of the movement range. Fig. 7 shows the paths of the ankle center in the x-y plane when the quadratic coefficient a_B is changed. At $a_B = 0$, a linear motion is obtained. As a_B becomes larger, convex motion becomes more prominent. The displacement in the z-axis direction is always set to be zero because the ankle center scarcely moved in this direction during anteroposterior movement in the previous study [21].

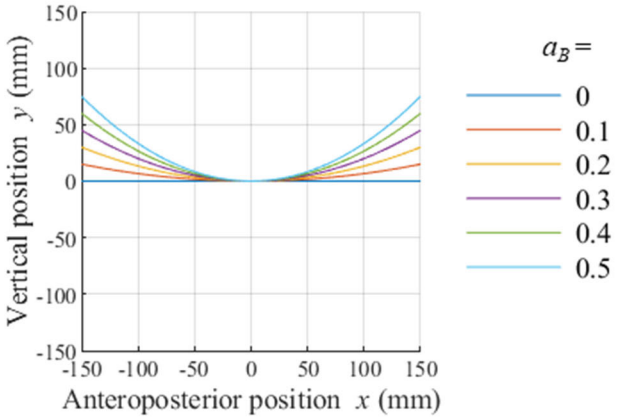

FIGURE 7. Paths of the ankle center in the x-y plane when the quadratic coefficient a_B is changed for anteroposterior movements.

Here, the velocity of the ankle center $v(t)$ is explained. In this study, a bell-shaped velocity waveform is used as the movement velocity of the ankle. In general, it is known that the velocity of a hand or foot moving from one point to another assumes a bell-shaped velocity waveform [29]. Flash *et al.* measured the reaching movement of the human upper limb and showed that the velocity coincided with the model expressed by a quartic function [30]. This quartic function is given as

$$v(t) = 15\left(\frac{t}{t_0}\right)^2\left\{\left(\frac{t}{t_0}\right)^2 - 2\left(\frac{t}{t_0}\right) + 1\right\}. \quad (3)$$

Equation (3) is used for the movement velocity of the ankle center in this article. The movement time t_0 represents the time required for the movement in the anteroposterior, lateral, or vertical direction, for example, moving in the backward or opposite direction. The value of t_0 was set to 2.0 s in this analysis.

Next, the trajectory of the ankle center during lateral movement is defined by

$$\begin{cases} x(t) = (a_{LX}/L)z(t)^2 \\ y(t) = (a_{LY}/L)z(t)^2 \\ z(t) = \pm L(-1 + 2\int_0^t v(\tau)\,d\tau) \end{cases} \quad (0 \le t \le t_o), \quad (4)$$

where a_{LX} and a_{LY} are constants representing quadratic coefficients. The lateral movement is the movement mainly in the z-axis direction. The plus or minus sign in $z(t)$ represents the direction of movement from right to left and from left to right, respectively. The experimental results of the previous study showed that the path of the ankle center was a convex curve in both the x-axis (forward) direction and y-axis (downward) direction, and the equations of $x(t)$ and $y(t)$ are defined to express this characteristic. Fig. 8(a) shows the paths of the ankle center in the z-x plane when the quadratic coefficient a_{LX} is changed, while Fig. 8(b) shows those in the y-z plane when the quadratic coefficient a_{LY} is changed. At $a_{LX} = 0$ and $a_{LY} = 0$, a linear motion is obtained.

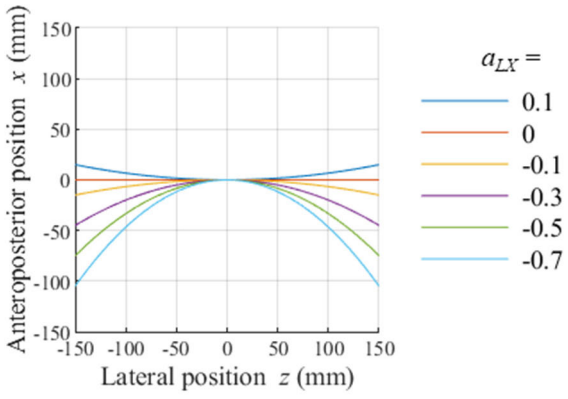

(a) Paths of the ankle center in the z-x plane when the quadratic coefficient a_{LX} is changed.

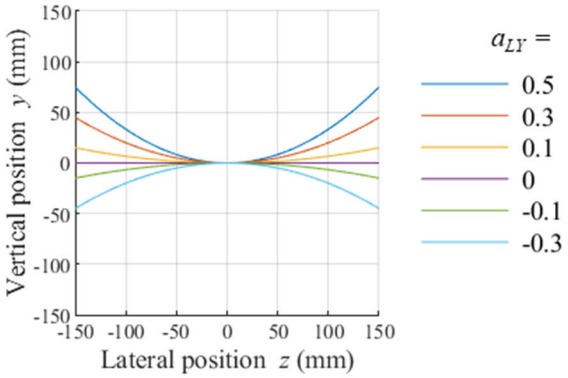

(b) Paths of the ankle center in the y-z plane when the quadratic coefficient a_{LY} is changed.

FIGURE 8. Changes in the center trajectory of the ankle when changing the quadratic coefficient for lateral movement.

In vertical movement, the trajectory of the ankle center is defined as

$$\begin{cases} x(t) = (a_U/L)y(t)^2 \\ y(t) = \pm L(-1 + 2\int_0^t v(\tau)\,d\tau) \\ z(t) = 0 \end{cases} \quad (0 \le t \le t_o), \quad (5)$$

where a_U is a constant representing the quadratic coefficient. The plus or minus sign in $y(t)$ represents upward or downward movement, respectively. Here, we deal with the curved motions where the path of the ankle center are convex in the x-axis (forward) direction. Fig. 9 shows the paths of the ankle center in the x-y plane when the quadratic

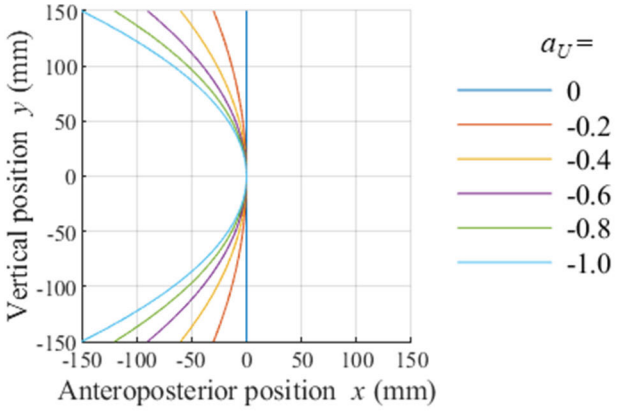

FIGURE 9. Paths of the ankle center in the *x-y* plane when the quadratic coefficient a_U is changed for vertical movement.

coefficient a_U is changed. At $a_U = 0$, a linear motion is obtained. The displacement in the z-axis direction is always set to be zero because the ankle center scarcely moved in the z-direction during vertical movement in the previous study.

Finally, we discuss the movement of the knee. As described above, the trajectory of the ankle center is determined by fixing the position of the hip joint in the coordinate system. However, the position of the knee in the lateral direction is not uniquely predetermined, so it is necessary to define it. As shown in Fig. 10, the analysis of the lateral movement requires that the knee must move in a lateral direction in step with the movement of the ankle center. Concretely, it is assumed that the position in the z-axis direction of the knee joint center is always proportional to the position in the z-axis direction of the ankle center, and we set the ratio between them as R_L. When the ratio $R_L = 0$, the lateral movement of the ankle center is accomplished by the external or internal rotation of the hip joint, as shown in Fig. 11. Whereas, when the ratio $R_L = 1$, the lateral movement is mainly performed by the abduction or adduction of the hip joint, as shown in Fig. 12. By taking the ratio R_L as an analysis parameter, various movements involving the knee can be analyzed. In the

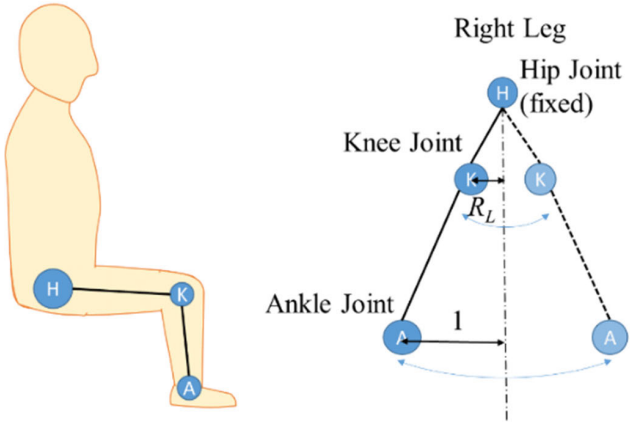

FIGURE 10. Relation between the lateral positions of the ankle and knee.

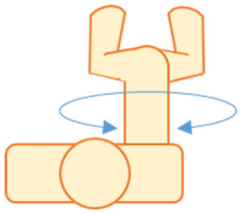

FIGURE 11. When the ratio $R_L = 0$, lateral movement of the ankle center is produced by the external or internal rotation of the hip joint.

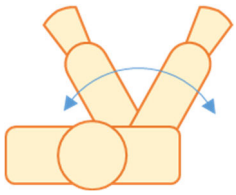

FIGURE 12. When the ratio $R_L = 1$, lateral movement of the ankle center is produced mainly by the abduction or adduction of the hip joint.

anteroposterior and vertical movement, the displacement in the z-axis direction of the knee joint center is always set to be 0.

The parameters used in the analysis are shown in Table 1. The analysis was carried out by varying a_B for anteroposterior movement; a_U for vertical movement; and a_{LX}, a_{LY}, and R_L for lateral movement.

TABLE 1. Parameters of motion as input for leg musculoskeletal analysis.

Parameter	Symbol	Range
Quadratic coefficient in the y-axis direction of the anteroposterior movement	a_B	$0 \le a_B \le 0.5$
Quadratic coefficient in the x-axis direction of the lateral movement	a_{LX}	$-0.7 \le a_{LX} \le 0.1$
Quadratic coefficient in the y-axis direction of the lateral movement	a_{LY}	$-0.3 \le a_{LY} \le 0.5$
Ratio of knee and ankle movements in lateral movements	R_L	$0 \le R_L \le 1.0$
Quadratic coefficient in the x-axis direction of the vertical movement	a_U	$-1.0 \le a_U \le 0$

III. RESULTS AND DISCUSSION OF MUSCULOSKELETAL ANALYSIS OF LEG MOTION

This section presents and discusses the results of the musculoskeletal analysis explained in Section II.

A. ANTEROPOSTERIOR MOVEMENT

Fig. 13 shows the analysis results of anteroposterior movements by the plot of E_{me} against the quadratic coefficient a_B. The solid curve shows the result when the ankle center is moved forward, and the dashed curve shows the result when the ankle center is moved backward. Fig. 13 indicates that E_{me} initially decreases as a_B increases from 0 to 0.18, where E_{me} becomes minimum, but then increases as a_B increases. As compared with the case of linear motion ($a_B = 0$),

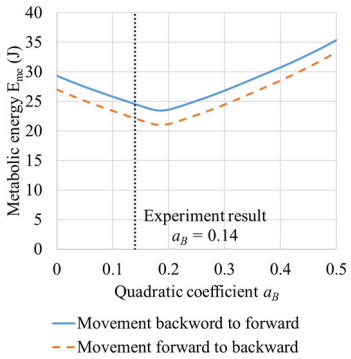

FIGURE 13. Analysis results of the relation between E_{me} and the degree of convexity of the path in the anteroposterior movement.

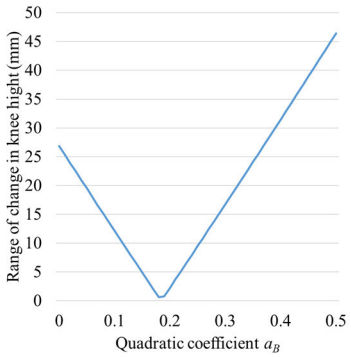

FIGURE 14. Range of change in knee height during movement from forward to backward.

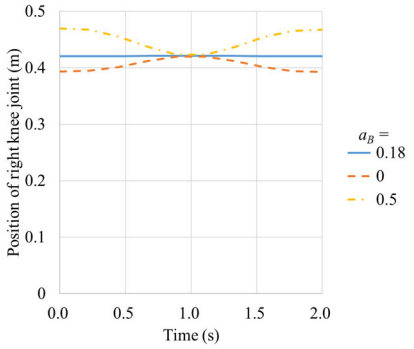

FIGURE 15. Changes in the vertical position of the knee joint during movement with time.

the value of E_{me} at $a_B = 0.18$ is as large as 77.9% during backward movement and 79.9% during forward movement. Thus, the values of E_{me} at $a_B = 0.18$ are smaller than those at $a_B = 0$ by more than 20%. Therefore, the muscle load is smaller as the ankle center moves, while it increases to a convex shape in the downward direction rather than following a linear shape in the anteroposterior direction. Namely, it is verified that the movement characteristic measured in the experiment can be qualitatively explained by the first hypothesis in Section II.A.

Next, we discuss whether the ankle center movement that minimizes the muscle load given in Fig. 13 coincides with the movement measured in the experiment of the previous study [21]. The analysis result shows that the quadratic coefficient a_B for the minimum E_{me} is 0.18, as explained above, whereas the average of the quadratic coefficient a_B is about 0.14 (SD = 0.06) in the experimental results, as shown by the dotted line in Fig. 13. The value of the quadratic coefficient $a_B = 0.14$ is closer to $a_B = 0.18$ for the minimum E_{me} than to $a_B = 0$ for the linear motion. At the same time, the value of E_{me} at $a_B = 0.14$ is also closer to the minimum E_{me} than the E_{me} value in the linear motion. Thus, it is suggested that the test subjects performed a motion close to the motion that produced the minimum muscle load. Therefore, it is shown that the movement characteristic measured in the experiment can be also quantitatively explained by the first hypothesis in Section II.A.

Now, we discuss the reason why E_{me} changes as shown in Fig. 13. Fig. 14 shows the range of change in knee height during anteroposterior movement for each value of a_B. Fig. 15 shows changes in the vertical position of the knee joint against time at $a_B = 0, 0.18$, and 0.5. Figs. 14 and 15 show that the knee height hardly changes at $a_B = 0.18$. This means that only the distal side of the knee joint moves without using the hip joint when $a_B = 0.18$. The muscle load is considered to be minimized at $a_B = 0.18$ because the upper leg does not need to move. However, the knee height changes when a_B is smaller or larger than 0.18 in Fig. 15 because it is necessary to move not only the knee joint but also the hip joint to move the upper leg up and down in these movements. As a result, the muscle load becomes larger than the case of $a_B = 0.18$.

Here, we discuss the relation between the quadratic coefficient $a_B = 0.14$ corresponding to the path obtained in the experiment and $a_B = 0.18$, where E_{me} takes the minimum value. The experimental result of $a_B = 0.14$ is significantly smaller than $a_B = 0.18$ with a significance level of 5%. This means that the path of the ankle center in the experimental results is slightly closer to the linear line than in the case of the minimum E_{me}. This suggests that the test subjects might perform a curved motion that was slightly close to a linear motion because they intended a linear motion and the difference in the path between the linear motion and the motion with the minimum muscle load was too large to be negligible.

B. LATERAL MOVEMENT

1) CHANGE IN E_{ME} WITH FIXED RATIO R_L

Fig. 16 shows the analysis results of E_{me} for lateral movement. Each panel in Fig. 16 shows a contour plot of E_{me} with the quadratic coefficient in the x-axis direction a_{LX} on the horizontal axis and the quadratic coefficient in the y-axis direction a_{LY} on the vertical axis. The analysis was carried out by changing the ratio R_L in increments of 0.1, and typical results are shown in Fig. 16(a)–(f).

In each plot, the globally minimum point of E_{me} for the changes in the quadratic coefficients a_{LX} and a_{LY} is indicated by a solid red circle. If a_{LX} and a_{LY} increase or decrease from this point, the value of E_{me} monotonically increases. When the ratio R_L is fixed, we call the quadratic coefficients for the

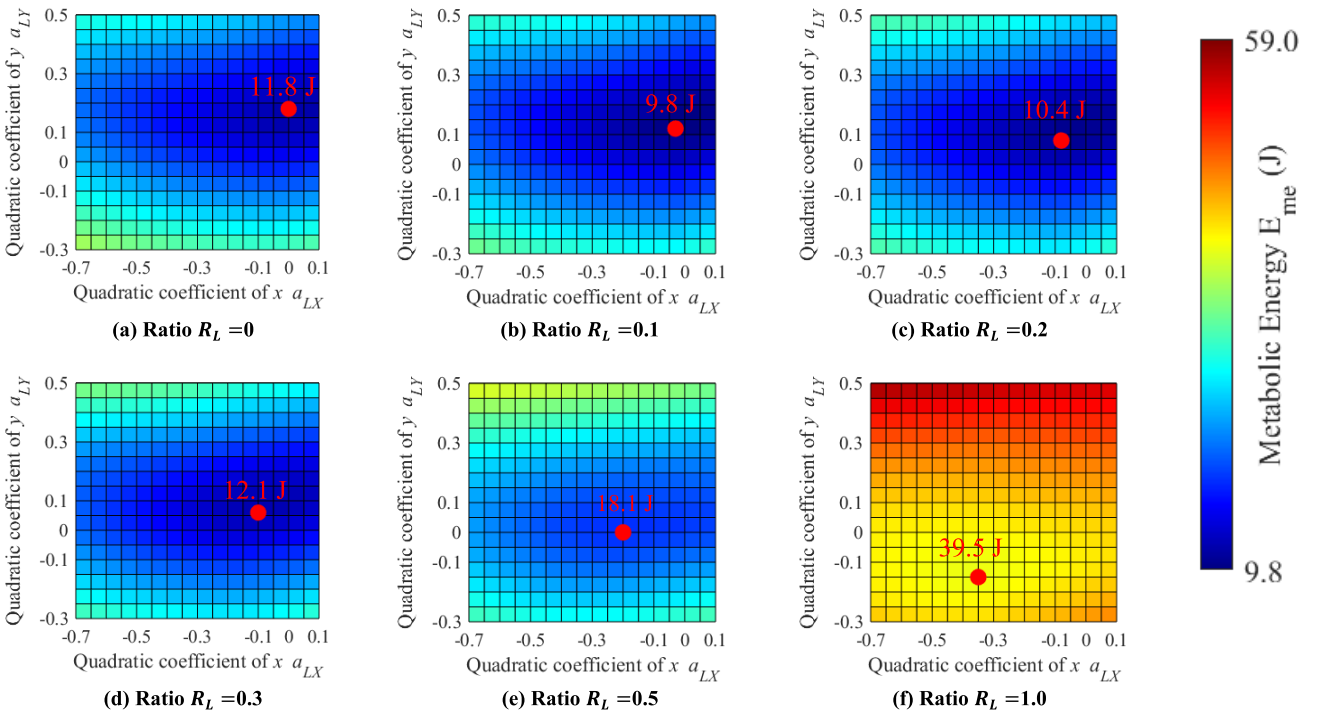

FIGURE 16. Analysis results of the relation between the quadratic coefficients a_{LX}, a_{LY}, and E_{me} in the lateral movement. Solid red circles indicate the minimum value (optimum coefficient) in each graph.

minimum E_{me} the optimum coefficients at the ratio R_L. Here, we focus on the graphs of $R_L = 0$ to 0.5, excluding $R_L = 1.0$ where E_{me} is remarkably large. In these graphs, a_{LX} is 0 or less and a_{LY} is 0 or more at the optimum coefficients indicated by the red circle. More specifically, a_{LX} is negative and a_{LY} is positive for $R_L = 0.1$, 0.2 and 0.3; a_{LX} is 0 and a_{LY} is positive for $R_L = 0$; and a_{LX} is negative and a_{LY} is 0 for $R_L = 0.5$. Therefore, when the ankle center is moved in the lateral direction, the muscle load takes a minimum in a curved motion whose path is convex in the forward and downward directions. The linear motion corresponds to the situation where both a_{LX} and a_{LY} are 0, but the muscle load at the linear motion is larger than that at the optimum coefficients. This supports the consistency of the first hypothesis explained in Section II.A. It is noted that E_{me} at the optimum coefficients takes the minimum value at $R_L = 0.1$. Also, at $R_L = 0$ to 0.5, the value of E_{me} at the optimum coefficients is smaller by about 3.1% to 23.8% than that of E_{me} in the case of linear motion.

2) EFFECT OF QUADRATIC COEFFICIENTS WITH FIXED RATIO R_L

As described above, there are optimum coefficients at which E_{me} is minimized against a_{LX} and a_{LY} for any ratio R_L. Here, we discuss what these optimum coefficients depend on. In Fig. 17, the solid and dashed red curves show the condition where the total vertical knee movement distances are 50 mm and 20 mm, respectively. The solid and dashed blue curves show the condition where the total knee flexion angle is 10° and 2°, respectively. Focusing on $R_L = 0$ to 0.5, the point of the optimum coefficients is located in the area where the total vertical knee movement distance is small and the total knee flexion angle is also small in each figure. Therefore, it is proven that E_{me} minimized when both the hip joint flexion/extension and the knee joint flexion/extension are small for $R_L = 0$ to 0.5. The hip joint can perform three kinds of motions, which are the flexion/extension, abduction/adduction shown in Fig. 12 and the external/internal rotation shown in Fig. 11, but abduction/adduction and external/internal rotation do not significantly affect the relative distribution of E_{me}. The reason is considered to be as follows. The lateral movement of the ankle center is mainly performed by a combination of abduction/adduction and external/internal rotation of the hip joint: mainly by the external/internal rotation when the ratio R_L is around 0, mainly by the abduction/adduction when the ratio R_L is around 1, and by the combination of those motions when the ratio R_L is between 0 and 1. Thus, when the ratio R_L is fixed, the changes of the external/internal rotation and the abduction/adduction are small as the quadratic coefficient changes. Therefore, the external/internal rotation and abduction/adduction may not affect the relative distribution of E_{me} in Fig. 16.

Hip joint flexion/extension and knee joint flexion/extension are considered to be the main factors that produce the muscle load when the external/internal rotation and abduction/adduction are nearly constant. Then, the muscle load becomes small when the amounts of the hip joint flexion/extension and knee joint flexion/extension are small in each panel of Fig. 16.

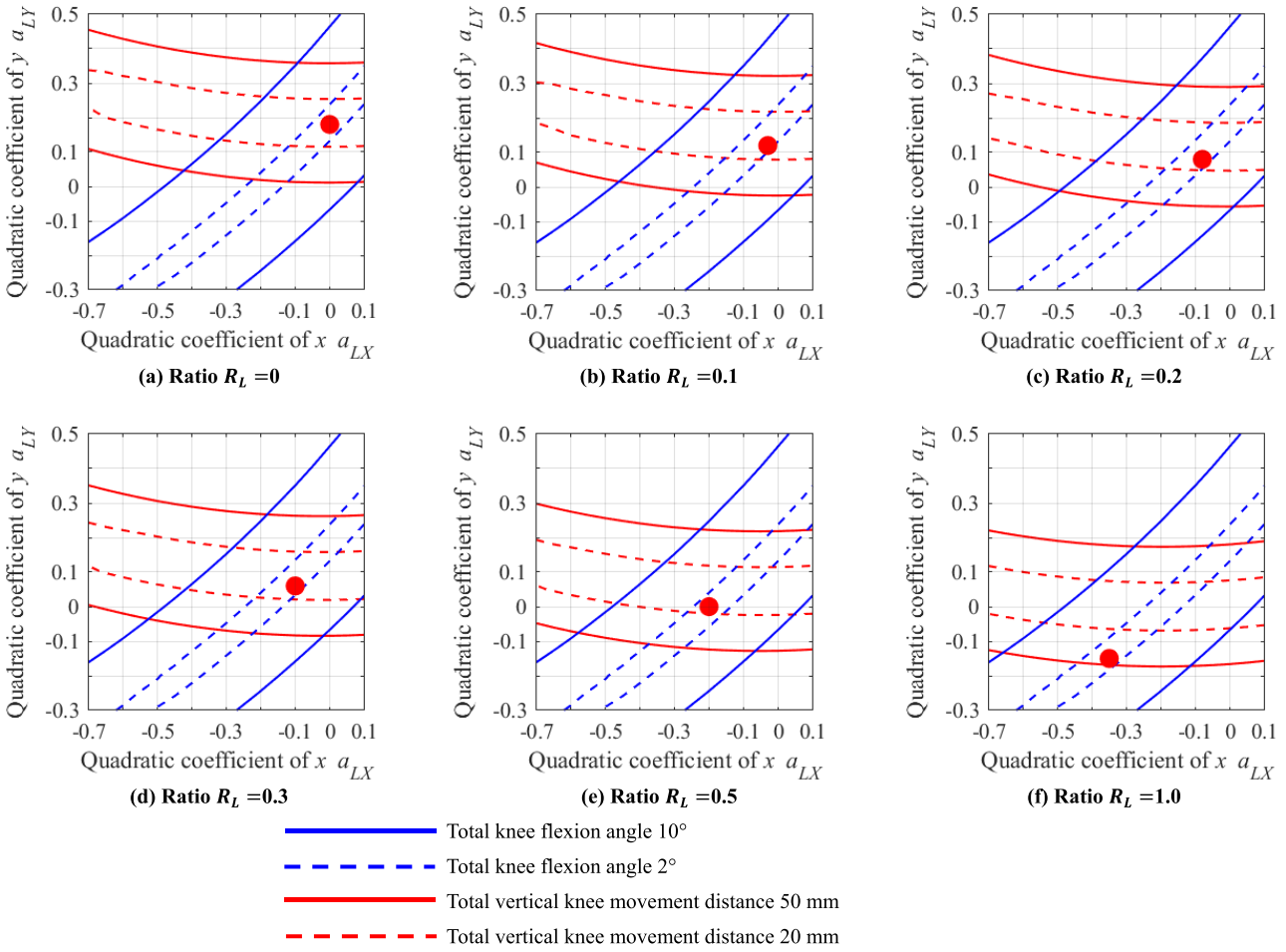

FIGURE 17. Analysis results of the relationship between the quadratic coefficients a_{LX} and a_{LY} and the total vertical knee movement distance and the total knee flexion angle in the lateral movement. Solid red circles indicate the optimum coefficients.

3) ANALYSIS AND DISCUSSION OF THE EFFECT OF R_L

Fig. 18 shows the value of E_{me} when the ratio R_L is changed under the linear motion $(a_{LX}, a_{LY}) = (0, 0)$ and the optimum coefficients. The value of E_{me} tends to be small when R_L is small, such as 0.1 or 0.2, and to be large when R_L is larger.

We discuss the reason for this tendency. When the ratio R_L is small, the external/internal rotation of the hip joint is mainly performed as shown in Fig. 11. In contrast, when the ratio R_L is large, the abduction/adduction of the hip joint is mainly performed as shown in Fig. 12. The value of E_{me} is 12.2 J when movement is performed only with the external/internal rotation of the hip joint and without the abduction/adduction or the flexion/extension approximately corresponding to $R_L = 0$, $a_{LX} = 0$, and $a_{LY} = 0.2$. The value of E_{me} is much larger, 41.6 J, when movement is performed only with the abduction/adduction of the hip joint and without the external/internal rotation or flexion/extension corresponding approximately to $R_L = 1, a_{LX} = -0.2$, and $a_{LY} = 0$. Therefore, the muscle load during external/internal rotation of the hip joint is considered to be smaller than that during abduction/adduction. This may be because the mass of the body part moved by the hip joint muscle is smaller in the external/internal rotation than in the abduction/adduction. As a result, the tendency can be described as "the value of E_{me} tends to be small when R_L is small, such as 0.1 or 0.2, and large when R_L is large."

4) COMPARISON OF ANALYTICAL AND EXPERIMENTAL RESULTS

In the experimental results of the previous study [21], the average value of the ratio R_L was about 0.52(SD = 0.24), and the average values of the quadratic coefficients were $a_{LX} = -0.09$ (SD = 0.04) and $a_{LY} = 0.09$ (SD = 0.05) in the lateral movement. At the point of $a_{LX} = -0.09$ and $a_{LY} = 0.09$, the total vertical knee movement distance is close to 0 and the total knee joint flexion is close to 0°, as shown in Fig. 17(e). This is the result of analysis with $R_L = 0.5$, which is close to the ratio $R_L = 0.52$. In this respect, the test subjects seemed to perform a movement that minimizes the muscle load under the condition of this ratio R_L in the experiment.

Next, the experimental and analytical results are compared concerning the ratio R_L. Fig. 18 shows that the muscle load takes the minimum at the ratio R_L around 0.1 and 0.2, but the muscle load is larger at the ratio $R_L = 0.52$, corresponding to the experimental result. We now discuss the reason for this difference by considering the method of moving the ankle center linearly in the lateral direction in the cases of $R_L = 0$ and $R_L = 1$. Because the external/internal rotation of the hip joint is mainly performed when $R_L = 0$, the ankle center is also displaced in the vertical direction. It is necessary to use the flexion of the hip joint to compensate for this vertical displacement. In contrast, at $R_L = 1$, the ankle center is also displaced in the anteroposterior direction because the motion is mainly abduction/adduction. To compensate for this displacement, flexion of the knee joint is required. Consideration of these two conditions simultaneously suggests that it is difficult to perform a precise motion when $R_L = 0$ in comparison with $R_L = 1$, where only the lower leg is moved by flexion/extension of the knee joint, whereas the whole leg needs to be moved by flexion/extension of the hip joint at $R_L = 0$. Therefore, the test subjects might perform a motion close to $R_L = 1$ when they intend to perform a precisely linear motion of the ankle center in the lateral direction. Considering these facts, the ratio R_L of about 0.5 is an effective value for moving the ankle center as precisely as possible and for reducing the muscle load of the whole lower limb when the test subjects perform a movement close to the intended linear movement. This may be the reason why the test subjects chose the ratio $R_L = 0.52$ in the experiments of the previous study [21].

C. VERTICAL MOVEMENT

Fig. 19 shows the analysis results of E_{me} for vertical movement. When a_U decreases from 0, E_{me} initially decreases, reaches a minimum at $a_U = -0.18$, and then increases as a_U decreases. Thus, the muscle load is smaller when the ankle center moves slightly forward to create a convex motion rather than moving linearly in the vertical direction. However, the difference between the minimum value of E_{me} and the value of E_{me} in the linear motion is less than 10%, which is not as large. This result agrees with the second hypothesis explained in Section II.A. Also, the average of the quadratic coefficient of the curved motion a_U obtained by the previous study was -0.04(SD $= 0.07$), and the value of E_{me} is smaller than the linear motion, as shown in Fig. 19. Although the difference is not significant, the quadratic coefficient $a_U = -0.04$ of the experimental result is smaller than the quadratic coefficient $a_U = 0$ of the linear motion. This suggests that the test subjects may have performed a curved motion with a slightly smaller muscle load despite the intended linear motion.

Next, we discuss the reason why E_{me} changes when the quadratic coefficient a_U changes as shown in Fig. 19. Fig. 20 shows the schematic movement of the knee in the vertical direction while the lower leg remains vertical. This condition corresponds to $a_U = -0.19$, which is close to

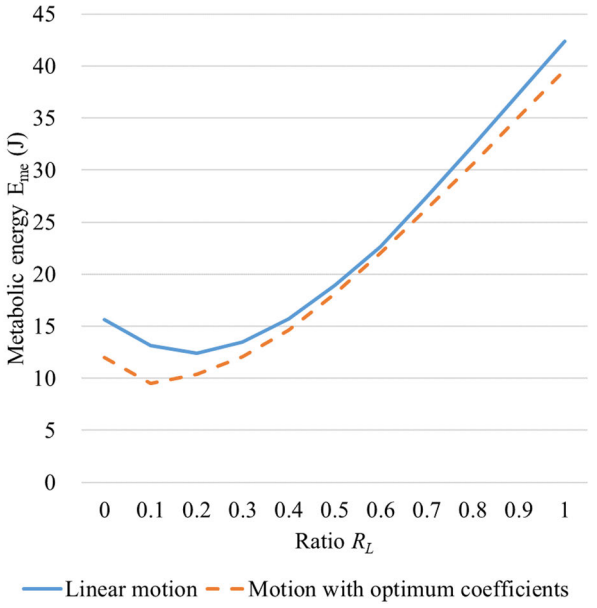

FIGURE 18. Values of E_{me} of the linear motion and the motion with optimum coefficients.

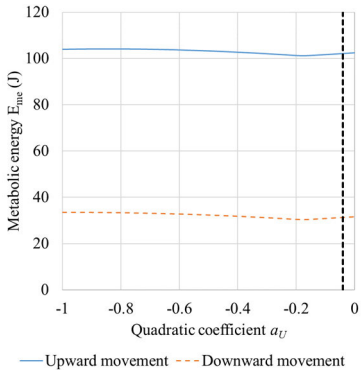

FIGURE 19. Analysis results of the muscle load during vertical movement.

$a_U = -0.18$ for the minimum E_{me} in Fig. 19. When the knee joint is moved up and down passively without applying force to it, this movement can be performed because the lower leg naturally remains vertical due to gravity. This movement creates little muscle load on the knee joint. In contrast, it is necessary to actively move the knee joint at a_U for other motions, which causes a larger muscle load on the knee joint. Therefore, the minimum E_{me} may occur around $a_U = -0.18$, as shown in Fig. 19.

IV. PROPOSED LEG SUPPORT DEVICE

According to the results of the analysis in the previous section, humans tend to move their lower limbs by following the path with less muscle load unconsciously when they operate a device with their lower limbs. Thus, an operating environment with less muscle load is desirable for the operator. Especially when operating a device by changing the position of the foot, it is necessary to keep the lower limbs suspended

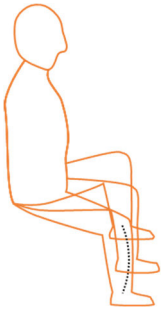

FIGURE 20. Raising and lowering the knee while keeping the lower leg vertical. The dotted line shows the trajectory of the center of the ankle joint.

in the air, as shown in Fig. 1, for a long time. Because the mass of the lower limb is large, the effect of gravity is also large. However, there are few situations in which the lower limb is kept suspended in daily life. Therefore, lifting the lower leg causes a large physical burden, which is a problem for realizing robotic operation with leg motion. To solve this problem, we propose a leg support device in this section. We first propose the concept of the device, and then analyze its output characteristics. After that, the development and experimental evaluation of two prototypes are described.

A. CONCEPT OF PROPOSED LEG SUPPORT DEVICE

First, we discuss which part of the lower limb should be supported by a leg support device. Here, we address the lower leg below the knee and the upper leg above the knee separately. In the case of the lower leg, the advantage is that the device can support the weight of both the upper and lower legs. However, because the range of motion of the lower leg is wider than that of the upper leg during device operation, the size of the device can be a disadvantage. The upper leg support has the opposite advantages and disadvantages. That is, it is an advantage that the device is easily kept small because the moving range of the upper leg is small, and it is a disadvantage that lower leg cannot be supported.

From the experience of our research so far, we recognize that the physical burden of device operation using leg motion is due to holding the upper leg in a suspended state. Also, it is recognized empirically that the physical burden is smaller when moving the lower leg than when moving the upper leg. According to the results of the analysis in Section III, it is easy to make E_{me} small when the vertical movement of the knee is made small during anteroposterior and lateral movements. It was also shown that when the ratio R_L is a small value, such as 0.1, it is easier to reduce E_{me} when moving only the lower leg from side to side as shown in Fig. 11 rather than when moving the upper leg from side to side as shown in Fig. 12. From these facts, it can be understood that the physical burden of moving the upper leg is larger than that of moving the lower leg. Considering also that a small device size is desirable, an upper leg support was adopted as the overall design premise in this study.

Next, the method for generating the leg supporting force is discussed. We considered an active system using motors and a passive system using a spring. In this study, the latter method was adopted because an active system requires motors, sensors, and control systems, and the system becomes complicated. In contrast, a passive system can be simple, and its fundamental effectiveness is easy to confirm.

Another requirement for the leg support device is that it cannot obstruct the operator's field of view or interfere with upper limb motion. Therefore, when the operator is in the posture shown in Fig. 1, no part of the leg support device should be in front of the operator's body above the waist. Thus, the leg support device has to be located within the space under the chair that the operator sits on or within the space next to the operator and below the waist level.

B. HIP FLEXION MOMENT

To discuss the output force of the leg support device, we calculated the hip flexion moment required to suspend the lower limb in the air. This is because the analysis in Section III showed that a major burden is caused by moving the upper leg in the vertical direction, that is, by flexing/extending the hip joint. Fig. 21 shows the results of the calculated hip flexion moment for the analytical model and conditions described in Section II when the ankle is moved from front to back, from left to right, and from down to up in 2 s. The graphs indicate that the value of the hip flexion moment changes during the movement of the leg in both linear and E_{me}-minimum motion. It is necessary to output a torque of the same value as the hip joint flexion moment to balance the output force of the leg support device with the weight of the lower limb perfectly. In this case, as shown in Fig. 21, the output force needs to be changed according to the movement of the lower limb. However, the system to realize this function may become complicated. In contrast, if the support output torque is close to, rather than exactly, the hip flexion moment, the system can be kept simple while still reducing the burden of the operator. Thus, the simpler approach was adopted. Fig. 21 shows that the value of the hip flexion moment is about 30 N·m for all movements. Therefore, we aimed to develop a leg support device that can generate a torque of about 30 N·m.

C. STRUCTURE OF LEG SUPPORT DEVICE

This article proposes two types of leg support device, and their structures are shown in Fig. 22. Fig. 22(a) shows the ''rotation'' type, in which the support that contacts the upper leg moves rotationally about a horizontal rotation axis that acts as a fulcrum, similar to the flexion/extension of the hip joint. When the hip joint center is set on the rotation axis, the support has the same movement as the rotation motion of the operator's upper leg. Note that different settings are possible. One end of the rotating link has the support surface that generates a supporting force F_{out}, and at the other end, a spring applies force F_{in}. Fig. 22(b) shows the ''vertical motion'' type, in which the support surface in contact with the upper leg moves vertically. The force F_{in} given by a spring acts on a wire and becomes converted into a force F_{out} pushing up the support part through a rod and rotary joint to

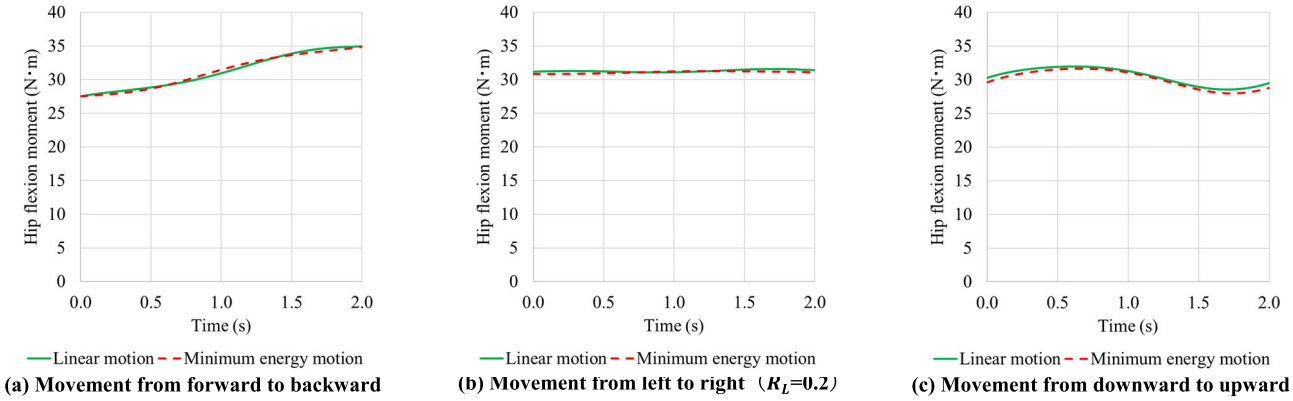

FIGURE 21. Calculated results of the hip flexion moment during each movement.

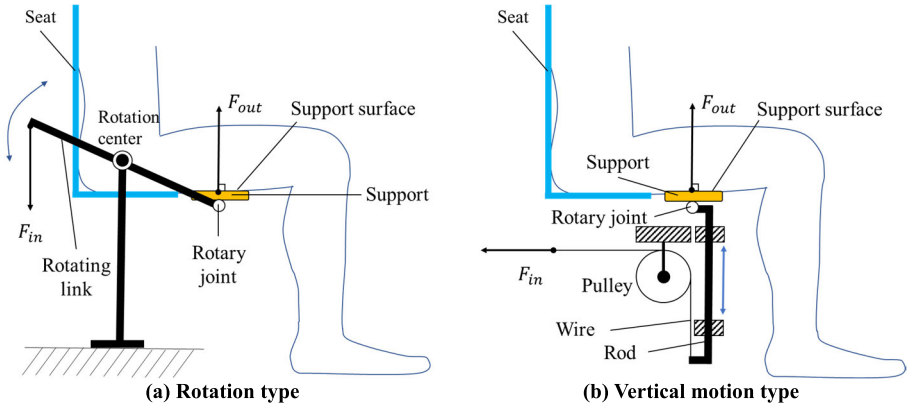

FIGURE 22. Schematic diagrams of the structure of the proposed leg support devices.

support the upper leg. The rotary joint is installed just below the support to passively change the posture of the support according to the movement of the upper leg.

Both the rotation and vertical motion types are designed as a system that pushes the upper leg up from underneath. Though a system that lifts the upper leg with a wire was also considered as another method for supporting the weight of the upper leg, this type of system was not adopted because the wire must be placed in front of the operator and may interfere with the operator's visual field and upper limb motion. A constant force spring is used for the proposed systems because both the rotation and vertical motion types need to output an approximately constant support force as the support surface moves.

Here, the rotation and vertical motion types are compared. The rotation type has a simple structure and few sliding parts, which leads to a small resistance in the movement. In contrast, the vertical motion type has an advantageous arrangement because this device can be located under the operator's chair, whereas the rotation type has a structure that protrudes to the side of the operator.

The developed leg support prototypes for the right leg are shown in Fig. 23. In the rotation type shown in Fig. 23(a), the main part of the device is arranged on the right side of the operator's chair and the support extends from the main structure. In the vertical motion type shown in Fig. 23(b), the main structure of the device is located under the chair of the operator. In both types, the support is larger than the average upper leg width in the lateral direction to support the leg even when it moves laterally.

D. ANALYSIS OF THE OUTPUT TORQUE OF PROPOSED LEG SUPPORT DEVICES

Equations (6) and (7) yield the supporting torque output by the rotation and vertical motion support types, respectively. As shown in Fig. 24, θ_1 is the flexion angle of the hip joint, d is the distance from the support surface to the upper leg axis, L is the distance from the center of the hip joint to the support surface in the upper leg axis direction, and L_0 is L when the operator is in the reference posture with the upper leg axis horizontal. In the rotation type, θ_2 is the rotation angle of the rotating link and the point (P_x, P_y) is the intersection between the action line of the supporting force F_{out} and the upper leg axis.

$$T = F_{out}L = \frac{F_{in}\sin(\pi + \theta_2 - \varphi)}{\cos(\theta_1 - \theta_2)}\sqrt{P_x^2 + P_y^2} \quad (6)$$

$$T = F_{out}L = \left(\frac{F_{in}}{\cos\theta_1}\right)\left(\frac{L_0}{\cos\theta_1} - d\tan\theta_1\right) \quad (7)$$

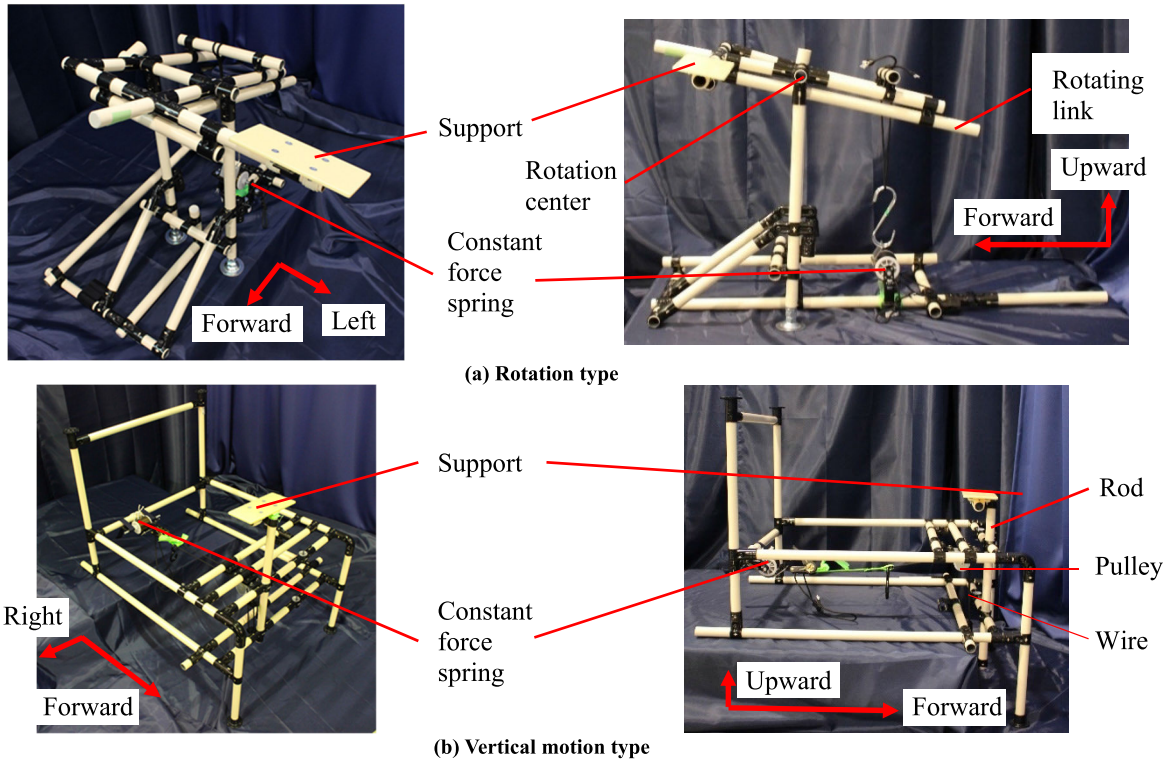

FIGURE 23. Developed leg support devices.

As shown in Fig. 24(a), the point O is set at the center of the hip joint and the O-XY coordinate system has point O as the origin, where the positive X-axis direction is forward and the positive Y-axis direction is upward. Here, P_x and P_y are obtained simultaneously by (8).

$$\begin{cases} P_y = P_x \tan\theta_1 \\ P_y\text{-}(c_y + l_1 \sin\theta_2) = -\dfrac{1}{\tan\theta_1}\{P_x - (c_x + l_1\cos\theta_2)\} \end{cases} \tag{8}$$

where (c_x, c_y) is the coordinate of the rotation center point of the rotating link C. Then, φ, the angle between the direction of the spring force F_{in} and the X-axis, is obtained by the following equation:

$$\varphi = \arccos \frac{l_2 - l_1\cos\theta_2 - l_4\sin\theta_2}{\sqrt{(l_2 - l_1\cos\theta_2 - l_4\sin\theta_2)^2 + (l_3 - l_1\sin\theta_2 + l_3\cos\theta_2)^2}}, \tag{9}$$

where l_1, l_2, l_3, and l_4 are the lengths shown in Fig. 24(a).

Fig. 25(a) shows the calculation results for the supporting torque of the rotation type given by (6). Here, the spring force of the constant force spring F_{in} is 133.8 N and $l_1 = 200$ mm, $l_2 = 220$ mm, $l_3 = 480$ mm, and $l_4 = 45$ mm are given based on the developed rotation type device. Also, we set $L_0 = 208$ mm and $d = 71.2$ mm. The calculation was performed at $(c_x, c_y) = (0, 0)$, $(30, 0)$, $(60, 0)$, $(0, -30)$, and $(0, -60)$. The result of $(c_x, c_y) = (0, 0)$ shows that the supporting torque changes against the hip joint flexion angle θ_1. This is because φ changes when θ_1 changes, which varies the relation between the direction of F_{in} and the longitudinal direction of the rotating link. At $(c_x, c_y) = (30, 0)$ and $(60, 0)$, the curve shape is almost the same as at $(c_x, c_y) = (0, 0)$, but the height of the curve, that is, the magnitude of the supporting torque, is different. This is because the distance L between the hip joint center point O and the support surface changes when c_x changes. In contrast, the slope of the curves of $(c_x, c_y) = (0, -30)$ and $(0, -60)$ differs from that of $(c_x, c_y) = (0, 0)$. This is because the distance L changes as the hip joint flexion angle θ_1 changes. These results indicate that the magnitude and the tendency of the supporting torque against θ_1 can be adjusted by changing c_x and c_y. This means that the supporting torque suitable for each operator can be obtained by changing c_x, that is, changing the position where the operator sits on the leg support device, although the required supporting torque differs depending on the operator because each operator has a different lower limb mass. The rotation type device has the advantage of being applicable to persons with various body sizes and weights without changing the structure of the device.

Fig. 25(b) shows the calculation results for the supporting torque of the vertical motion type given by (7). The calculation was performed at $L_0 = 178$ mm, 208 mm, and 238 mm. When the hip joint flexion angle θ_1 is in the range of $-20°$ to $10°$, the supporting torque decreases as θ_1 increases. This is because the position of the support surface along the upper leg axis approaches the hip joint as θ_1 increases. When L_0 is different, the torque curve is higher or lower because

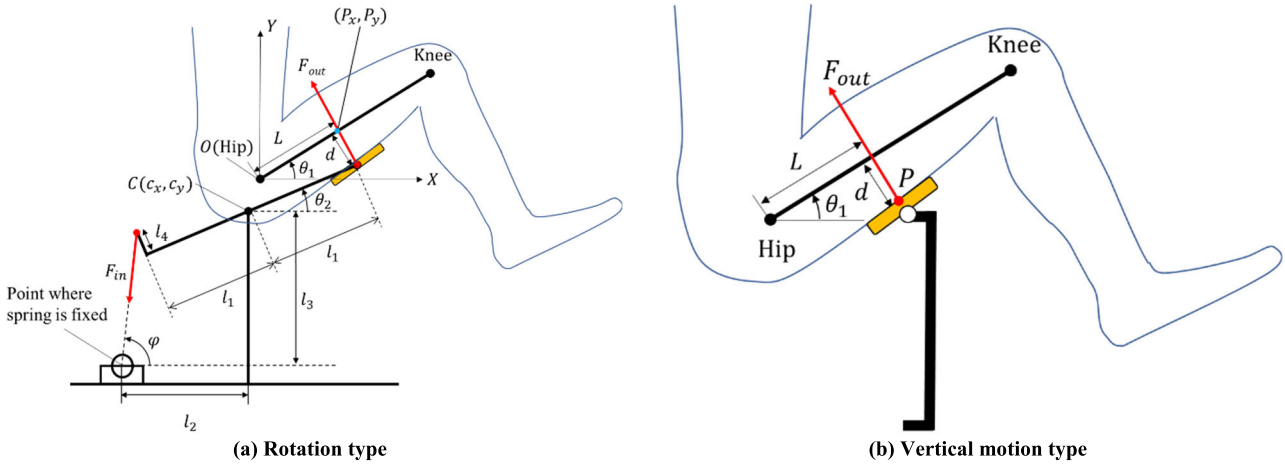

FIGURE 24. Variables for the analysis of supporting force of leg support devices.

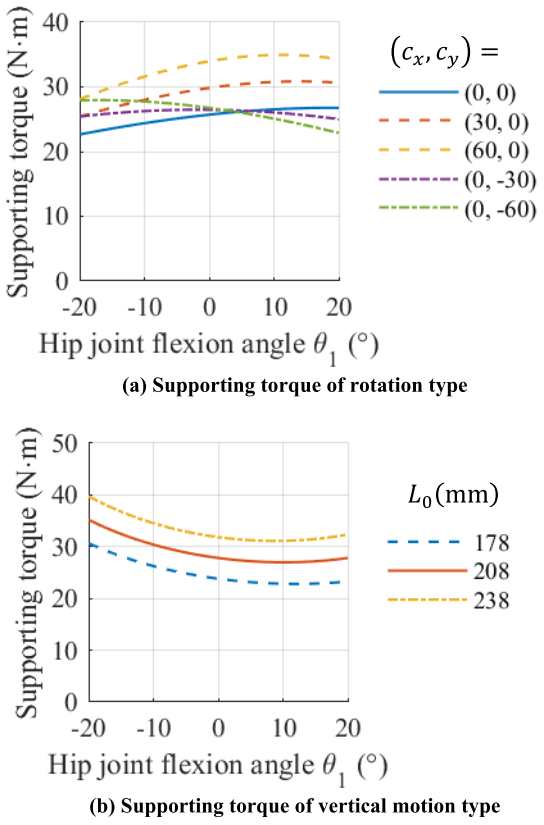

FIGURE 25. Theoretical values of supporting torque of leg support devices.

the moment arm length of the supporting torque is affected by L_0, that is, the distance between the hip joint center point O and the upper leg axis of the support surface in the reference posture. The vertical motion type device also has the advantage of being applicable to persons with various body sizes and weights without changing the structure of the device because the magnitude of the supporting torque against θ_1 can be adjusted by changing L_0.

Fig. 25 shows that the leg support devices can generate torque of about 30 N·m, which is the goal given in Section IV.B, by using the parameter conditions given here.

E. EXPERIMENT TO EVALUATE THE SUPPORTING FORCE OF THE DEVELOPED LEG SUPPORT DEVICES

An experiment to evaluate the supporting force characteristics of the proposed leg support devices was conducted by measuring the supporting force F_{out}. In this experiment, we measured the force perpendicular to the rotating link in the rotation type and the force parallel to the rod in the vertical motion type. The support was fixed not to rotate with respect to the rotating link axis or rod in this experiment. The measurement was performed by pressing down on a uniaxial force sensor (IMADA ZP-1000 N) as shown in Fig. 26. We reciprocated the support surface 10 times with a period of about 8 s in each set of measurements and conducted 10 sets of measurements for each leg support device. Also, the position of the support surface was measured by a real-time motion capture system (Claron Technology Inc., Micron Tracker H3-60).

Fig. 27 shows the average results over the entire trial of the rotation device and the theoretical output value. The larger the angle of the rotating link is, the larger the supporting force is. This tendency agrees with the theoretical behavior. In contrast, the magnitude of the supporting force is smaller than the theoretical value. This may be caused by friction between the moving parts of the device. As described above, the supporting torque can be changed by adjusting the position of the rod rotation center point C (c_x, c_y) to the hip joint center point O even when the supporting force is the same. Thus, the supporting force being different from the theoretical value does not present a problem for practical use.

Measurement results of the vertical motion device are shown in Fig. 28. We excluded data in the vicinity of the reversal point of upward/downward motion because the value changed rapidly in this region. The magnitude of the measured supporting torque is approximately constant in both

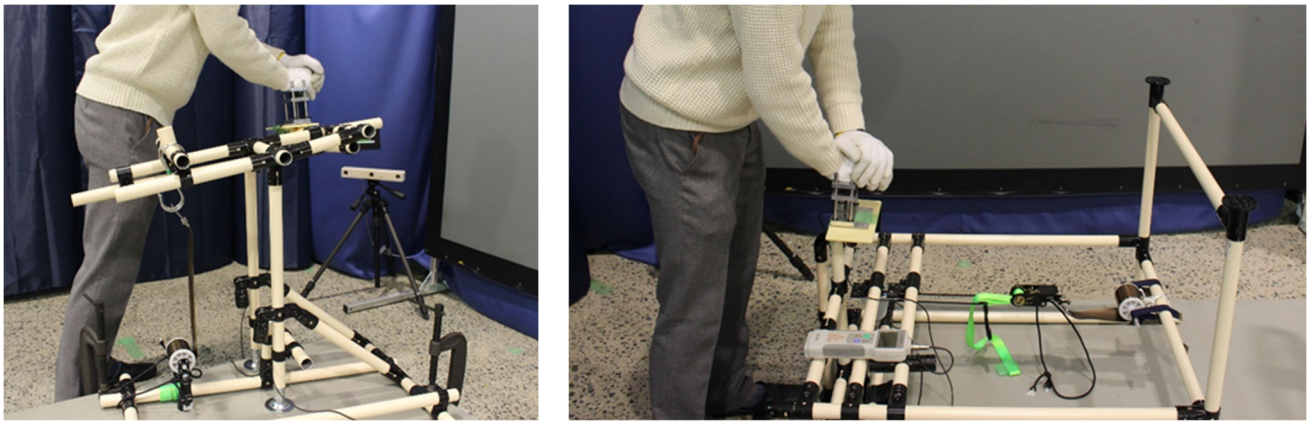

FIGURE 26. Experiment to measure supporting force of leg support devices.

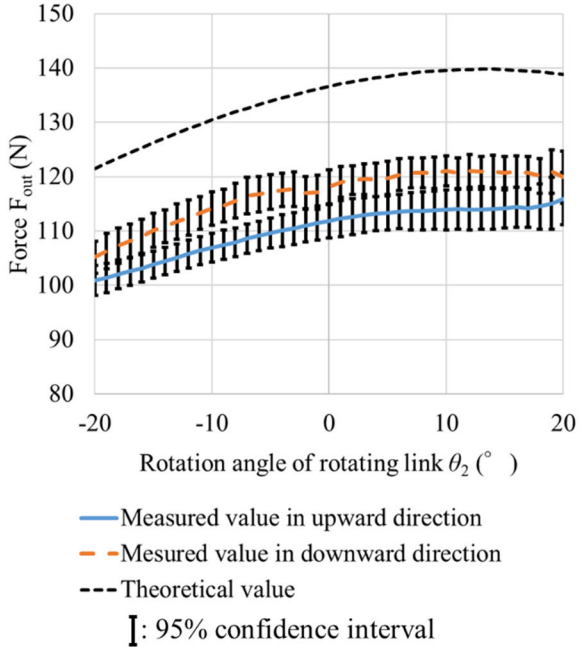

FIGURE 27. Measurement results of supporting force of the rotation type.

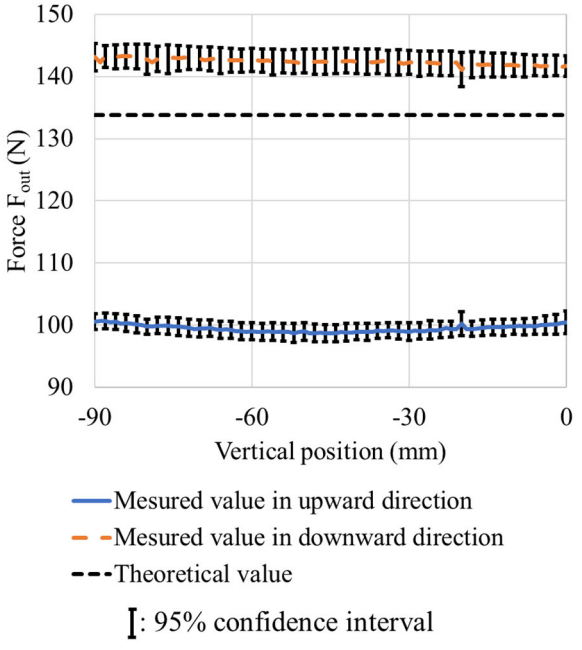

FIGURE 28. Measurement results of supporting force of the vertical motion type.

the upward motion and downward motion, which is the same tendency of the theoretical result. However, the measured values of the supporting force differ from the theoretical value. The measured values in upward and downward motions are greatly different, and the difference is larger than that of the rotation type. This may be because more moving parts, such as those supporting the rod, create friction in the vertical motion type than in the rotation type. As described above, the supporting torque can be changed by adjusting the contact position between the support surface and the upper leg even when the supporting force is the same. Again, the supporting force differing from the theoretical value does not present a problem in practical use. However, the supporting torque remains different between the upward and downward motion when the supporting force is different, which may affect the operator's use experience.

V. EVALUATION EXPERIMENT

This section discusses an experiment to evaluate the effectiveness of the leg support prototypes described in Section IV. The experiment was conducted with the approval of the Ethics Committee, Graduate School of Engineering, Kyoto University.

A. EXPERIMENTAL SETUP

As shown in Fig. 29, either the rotation or vertical motion type leg support device was arranged with a chair. A test subject sat on the chair with his or her right upper leg on the support

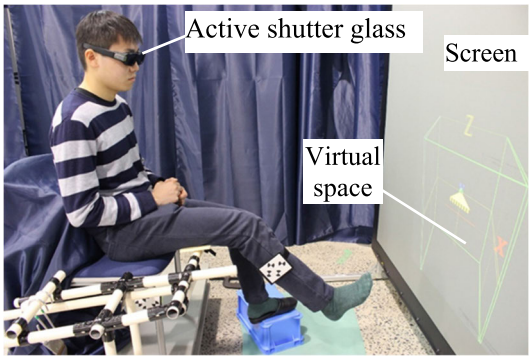

FIGURE 29. Experimental setup to evaluate the effectiveness of the leg support devices (rotation type shown).

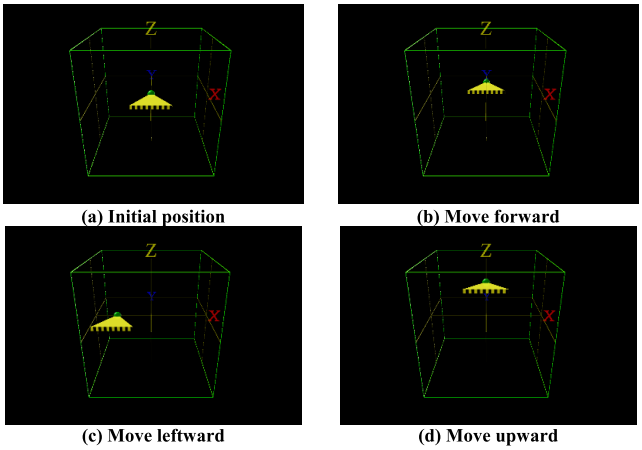

FIGURE 30. Initial position and states of reciprocating motions during operation of imaginary object.

surface of the device and right foot suspended in the air. A three-dimensional virtual space was displayed on a screen in front of the test subject. The IOO moved backward and forward, rightward and leftward, or upward and downward in the virtual space. The test subjects were asked to move their leg in the same way as the IOO with the assumption that they were operating the IOO with the position of their ankle center. The magnitude of the burden on the whole lower limb that the test subjects felt was evaluated by a questionnaire. For comparison, the same experiments were also conducted without any leg support device.

B. MOTION OF THE IMAGINARY OPERATED OBJECT

In this experiment, the virtual space and the IOO were used [17], [31]–[33]. The IOO was a yellow triangle with a green sphere fixed at its tip, as shown in Fig. 30(a). A green cubic frame was displayed in the virtual space to represent the range of motion of the IOO. The virtual space was viewed by the test subjects from the rear oblique upper side. To describe the virtual space and the IOO, software for three-dimensional space display (SOLIDRAY Ltd., Omega Space) was used. The virtual space was projected onto the screen by a specialized projector. The test subjects were able to see the virtual space stereoscopically using an active shutter glass (NVIDIA Corp., 3D VISION2).

As shown in Fig. 30(b) to (d), the IOO moved backward and forward, rightward and leftward, or upward and downward in the virtual space and made reciprocating motion with 11 round trips. The reciprocating motion of the IOO started after a countdown of 5 s.

C. METHOD FOR EVALUATING MUSCLE LOAD

In this experiment, the muscle load was evaluated by the magnitude of the subjective exercise intensity in the whole lower limb that the test subjects felt during each movement. A questionnaire based on the visual analogue scale method [17], [34] was conducted after each task was completed. The test subject was given a questionnaire on which a line without a scale was drawn and asked to place a mark on the line at the most suitable point corresponding to the test subject's effort, with the left and right ends of the line indicating "nothing at all" and "very, very strong (almost max.)," respectively. The distance from the left end of the line to the position marked by the test subject was converted to a point between 0 and 100 and used to evaluate the subjective exercise intensity. After finishing all tasks, the test subjects were asked to describe the difference in perception of exercise intensity and in the ease of foot movement from the following three aspects: between using and not using the leg support devices, among the three directions of the movements, and between the rotation and vertical motion types. Comments on other topics were also recorded if the test subjects had any.

D. EXPERIMENTAL PROCEDURE

The test subjects were 10 healthy adult men (mean age of 23.4 years, SD = 0.7) without injury or physical disabilities. Before each subject used a leg support device, we first obtained the supporting torque that maintained his upper leg in the horizontal reference posture defined in Fig. 6 without the subject applying his own force to his leg. Here, to address individual differences in the physical features of the test subjects, such as bodyweight, the anteroposterior position of the leg support device was adjusted for each test subject by adjusting the contact position between the supporting surface and the subject's upper leg. The test subjects were instructed to move their legs under the assumption that they were operating the three-dimensional position of the IOO corresponding to the position of the center of their right ankle. The test subjects were also instructed to start the movement from the reference posture.

Each test subject performed the tasks of anteroposterior movement, lateral movement, and vertical movement once under each condition of rotation type device, vertical motion type device, and no support device. The range of motion of the ankle center was restricted to about 300 mm in each of the anteroposterior, lateral, and vertical directions. To prevent the ankle center from deviating significantly beyond 300 mm, before each task the test subjects were shown the position of 300 mm on each side with a cuboid instrument.

The questionnaire was conducted after each task. The order of rotation type, vertical motion type, and no support and the order of the movement directions were determined randomly for each test subject to prevent the task order from affecting the results.

E. EXPERIMENTAL RESULTS AND DISCUSSION

Fig. 31 shows the questionnaire results for the subjective exercise intensity. The higher the value is, the greater the subject's exercise intensity was during the task, that is, the greater the burden on the body was. The evaluation values were compared by the non-parametric multiple tests using the Steel-Dwass method between each condition. Asterisks (∗) indicate cases where there was a significant difference at 5%. The results of the average of all movements at the left of the graph show that the evaluation value is lower by 55% for the rotation type device and by 50% for the vertical motion type device in comparison with the task without support, and there is a significant difference at 5%. Also, the evaluation values of movement in the anteroposterior, lateral, and vertical directions in the rotation and vertical motion types are significantly smaller than those without support. This indicates that the subjective body burden could be reduced to about half by the developed leg support devices. Therefore, the effectiveness of the leg support device was verified.

Next, we compared the rotation and vertical motion device types. Though the evaluation values for all movements and anteroposterior, lateral, and vertical movements showed no significant differences, the resultant values of the vertical motion type are slightly larger than those of the rotation type for all movements and for the lateral and vertical movements. Regarding the comments from the test subjects, all test subjects stated, ''There is a difference in the perception of the exercise intensity between the rotation type and the vertical motion type.'' Six of the test subjects stated, ''The rotation type is easier'' or ''The vertical motion type is more burdensome,'' and two other test subjects stated, ''The rotation type is easier than the vertical motion type for some movements and as easy as the vertical motion type for other movements.'' Overall, eight test subjects gave comments that rated the rotation type higher than the vertical motion type. Also, five of them commented, ''The rotation type is easier in the vertical direction motion'' or ''The vertical motion type is more burdensome in the vertical direction motion.'' In particular, three test subjects commented, ''It is necessary to push the support part strongly when moving from up to down in the vertical motion type.'' As described in Section IV.E, the difference in the supporting forces of the rotation type between upward motion and downward motion is small, but that of the vertical motion type is large. Also, the vertical motion type generates a large supporting force during downward motion. The test subjects might have perceived this characteristic.

Finally, the improvements in movements in the anteroposterior, lateral, and vertical directions were compared. Compared to no support, the average evaluation values of the subjective exercise intensity of the rotation type and vertical motion type are 44% for anteroposterior movement, 43% for lateral movement, and 53% for vertical movement. Though each case improves greatly compared to no support, the improvement is larger for the anteroposterior and lateral movements than that for the vertical movement. For the tasks without support, the muscle load becomes relatively large for maintaining the vertical position of the upper leg, even during the anteroposterior and lateral movements, though the hip joint flexion is small. Because it counteracts this kind of muscle load, the use of the leg support device is considered to achieve a large improvement in the subjective exercise intensity. During vertical movement, the vertical travel of the upper leg is relatively large. When the upper leg is moved downward, the moving direction and gravity direction are the same, making it easy to lower the leg without support. However, the support creates resistance to downward motion, and it is necessary to exert muscle force when lowering the leg when a support device is used. This might be the reason why the improvement in the vertical movement was smaller than that in the anteroposterior and lateral movements.

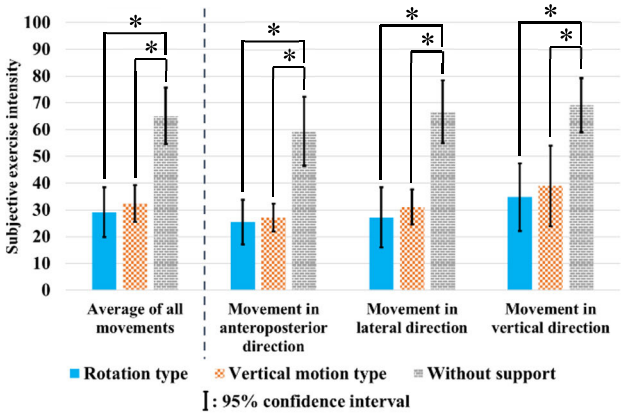

FIGURE 31. Evaluation results of subjective exercise intensity during the experiment (∗: $p < 0.05$).

VI. CONCLUSION

The master-slave operation method has the advantage of being easy to operate because an operator can manipulate a multi-DOF robot arm by only moving his or her body part. During operation of such devices, normally the upper limb is used, but the lower limb has a similar skeletal system. Thus, multi-DOF devices can be commanded by using a leg in the same manner as using an arm. However, multi-DOF operation by the lower limb has two problems: 1) Even when the operator intends to move a leg linearly, the leg actually moves in a curved motion when visual feedback is absent, and the reason is not clear. 2) It is physically burdensome to keep a foot suspended in the air for a long time during device operation. This study aimed to clarify and solve these problems. For problem 1), we assumed the reason is due partly to the muscle load and evaluated the muscle load of various leg motions quantitatively by a musculoskeletal analysis for three-DOF position manipulation. The following results were obtained:

1) In the anteroposterior movement, the required energy was about 20% less when the ankle center was moved convexly downward than when moved linearly because the upper leg does not need to be moved. Comparing the results of this analysis and an experiment in previous research showed that the movement performed by the test subjects intending a linear motion was close to the curved motion, where the required energy was minimized.
2) In the lateral movement, the muscle load was minimized when the motion curved convexly in the forward and downward directions and the necessary energy was smaller than the linear motion by about 3.1% to 23.8%. Comparing the results of the analysis and the experiment showed that the movement in the experiment was a curved motion that almost minimized the required energy when the knee/ankle lateral movement ratio R_L was 0.5.
3) In the vertical movement, it was shown that the muscle load was smaller when the ankle was moved slightly convexly in the forward direction rather than in a strictly linear motion. In this movement, the knee was moved up and down without exerting force on the knee joint. However, the difference in the required energy between the curved motion and the linear motion was about 10% or less, which was so small that the movement measured in the experiment did not always follow the curved path of the minimum energy.

This study also tackled problem 2) and proposed two device designs for supporting the lower limb during robot operation. The obtained results were as follows:

1) One leg support device proposed in this article is a rotation type in which the supporting surface for the upper leg rotates about a fulcrum like a seesaw, and the other is a vertical motion type in which the supporting surface can move vertically. Both leg support devices could support the upper leg with the force of a spring without obstructing the subjects' visual field or interfering with the ability to use their arms.
2) Calculation of the hip joint flexion moment showed that about 30 N·m of torque was necessary for supporting the leg. Theoretical equations of the output force of the proposed leg support devices were derived, and it was proved that the required torque could be generated by the developed devices. It was also shown that the devices could be applied to persons with various sizes and weights because suitable supporting torque could be obtained for each operator by changing the sitting position. Prototypes of the proposed devices were fabricated, and the supporting force output was measured. The results verified that the tendency of the output followed the theory qualitatively.
3) An effectiveness evaluation experiment was conducted, where test subjects moved their legs forward/backward, leftward/rightward, and upward/downward repeatedly. The results showed that the subjective exercise intensity decreased by 55% in the rotation type and by 50% in the vertical motion type compared with no support, which showed the effectiveness of the proposed leg support devices. The exercise intensity was 44% for anteroposterior movement, 43% for lateral movement, and 53% for vertical movement compared with movement without a support device.

In future work, we make the devices more practical for manipulation by the leg.

ACKNOWLEDGMENT

The authors would like to thank Mr. Harutaka Miyauchi of Kyoto University for his cooperation.

REFERENCES

[1] G. S. Gupta, S. C. Mukhopadhyay, and M. Finnie, "WiFi-based control of a robotic arm with remote vision," in *Proc. IEEE Intrumentation Meas. Technol. Conf.*, Singapore, May 2009, pp. 557–562.
[2] C. A. Arango, J. R. Martinez, and V. Z. Perez, "Master-slave system using Kinect and an industrial robot for teleoperations," in *Proc. Pan Amer. Health Care Exchanges (PAHCE)*, Medellin, Colombia, Apr. 2013, pp. 1–6.
[3] A. Shaikh, G. Khaladkar, R. Jage, and T. Pathak, "Robotic arm movements wirelessly synchronized with human arm movements using real time image processing," in *Proc. Texas Instrum. India Educators' Conf.*, Bengaluru, India, Apr. 2013, pp. 277–284.
[4] G. Du and P. Zhang, "Markerless human–robot interface for dual robot manipulators using Kinect sensor," *Robot. Comput.-Integr. Manuf.*, vol. 30, no. 2, pp. 150–159, Apr. 2014, doi: 10.1016/j.rcim.2013.09.003.
[5] C. P. Quintero, R. T. Fomena, A. Shademan, O. Ramirez, and M. Jagersand, "Interactive teleoperation interface for semi-autonomous control of robot arms," in *Proc. Can. Conf. Comput. Robot Vis.*, Montreal, QC, Canada, May 2014, pp. 357–363.
[6] M. Fuad, "Skeleton based gesture to control manipulator," in *Proc. Int. Conf. Adv. Mechatronics, Intell. Manuf., Ind. Autom. (ICAMIMIA)*, Surabaya, Indonesia, Oct. 2015, pp. 96–101.
[7] J. Grasshoff, L. Hansen, I. Kuhlemann, and K. Ehlers, "7DoF hand and arm tracking for teleoperation of anthropomorphic robots," in *Proc. ISR 47st Int. Symp. Robot.*, Münich, Germany, Jun. 2016, pp. 1–8.
[8] R. Mardiyanto, M. F. R. Utomo, D. Purwanto, and H. Suryoatmojo, "Development of hand gesture recognition sensor based on accelerometer and gyroscope for controlling arm of underwater remotely operated robot," in *Proc. Int. Seminar Intell. Technol. Its Appl. (ISITIA)*, Surabaya, Indonesia, Aug. 2017, pp. 329–333.
[9] D. Gong, J. Zhao, J. Yu, and G. Zuo, "Motion mapping of the heterogeneous master-slave system for intuitive telemanipulation," *Int. J. Adv. Robot. Syst.*, vol. 15, no. 1, pp. 1–9, 2018, doi: 10.1177/1729881417748134.
[10] M. Syakir, E. S. Ningrum, and I. Adji Sulistijono, "Teleoperation robot arm using depth sensor," in *Proc. Int. Electron. Symp. (IES)*, Surabaya, Indonesia, Sep. 2019, pp. 394–399.
[11] S. Chang, J. Kim, I. Kim, J. H. Borm, C. Lee, and J. Oh Park, "KIST teleoperation system for humanoid robot," in *Proc. IEEE/RSJ Int. Conf. Intell. Robots Syst. Hum. Environ. Friendly Robots High Intell. Emotional Quotients*, Kyongju, South Korea, Oct. 1999, pp. 1198–1203.
[12] G. S. Gupta, S. C. Mukhopadhyay, C. H. Messom, and S. N. Demidenko, "Master–slave control of a teleoperated anthropomorphic robotic arm with gripping force sensing," *IEEE Trans. Instrum. Meas.*, vol. 55, no. 6, pp. 2136–2145, Dec. 2006, doi: 10.1109/TIM.2006.884393.
[13] J. Rebelo and A. Schiele, "Master-slave mapping and slave base placement optimization for intuitive and kinematically robust direct teleoperation," in *Proc. 12th Int. Conf. Control, Autom. Syst.*, JeJu Island, South Korea, Oct. 2012, pp. 2017–2022.
[14] H. Lee, J. Kim, and T. Kim, "A robot teaching framework for a redundant dual arm manipulator with teleoperation from exoskeleton motion data," in *Proc. IEEE-RAS Int. Conf. Humanoid Robots*, Madrid, Spain, Nov. 2014, pp. 1057–1062.

[15] N. Tsujiuchi, K. Takayuki, and M. Yoneda, "Manipulation of a robot by EMG signals using linear multiple regression model," in *Proc. IEEE/RSJ Int. Conf. Intell. Robots Syst. (IROS)*, Sendai, Japan, vol. 2, Sep./Oct. 2004, pp. 1991–1996.
[16] P. K. Artemiadis and K. J. Kyriakopoulos, "EMG-based teleoperation of a robot arm in planar catching movements using ARMAX model and trajectory monitoring techniques," in *Proc. IEEE Int. Conf. Robot. Autom. (ICRA)*, Orlando, FL, USA, May 2006, pp. 3244–3249.
[17] M. Komori, T. Terakawa, and I. Yasuda, "Operability evaluation system and comparison experiment of gesture operation and button operation of robot manipulator," *IEEE Access*, vol. 8, pp. 24966–24978, 2020, doi: 10.1109/ACCESS.2020.2970761.
[18] Y. Huang, E. Burdet, L. Cao, P. T. Phan, A. M. H. Tiong, and S. J. Phee, "A subject-specific four-degree-of-freedom foot interface to control a surgical robot," *IEEE/ASME Trans. Mechatronics*, vol. 25, no. 2, pp. 951–963, Apr. 2020, doi: 10.1109/TMECH.2020.2964295.
[19] E. Abdi, M. Bouri, J. Olivier, and H. Bleuler, "Foot-controlled endoscope positioner for laparoscopy: Development of the master and slave interfaces," in *Proc. 4th Int. Conf. Robot. Mechatronics (ICROM)*, Tehran, Iran, Oct. 2016, pp. 111–115.
[20] M. Komori, T. Terakawa, and I. Yasuda, "Experimental investigation of operability in six-DOF gesture-based operation using a lower limb and comparison with that in an upper limb," *IEEE Access*, vol. 8, pp. 118262–118272, 2020, doi: 10.1109/ACCESS.2020.3002954.
[21] M. Komori and H. Miyauchi, "Position operation method by leg motion and characteristics of leg motion during operation," *J. Jpn. Soc. Design Eng.*, vol. 53, no. 7, pp. 511–526, 2018, doi: 10.14953/jjsde.2017.2773.
[22] D. Stambolian, M. Eltoukhy, and S. Asfour, "Development and validation of a three dimensional dynamic biomechanical lifting model for lower back evaluation for careful box placement," *Int. J. Ind. Ergonom.*, vol. 54, pp. 10–18, Jul. 2016, doi: 10.1016/j.ergon.2015.12.005.
[23] Y. Sun, C. Moore, and A. Nimbarte, "Musculoskeletal loading during dynamic two-wheeled cart pushing and pulling," in *Proc. 61st Annu. IIE Conf. Expo*, vol. 1, 2011, p. 1.
[24] Y. Hasegawa, S. Shimada, and K. Eguchi, "Wrist support device for a patient with muscle weakness (rehabilitation robotics and mechatronics)," in *Proc. JSME Annu. Conf. Robomec*, 2014, pp. 3P2-B03_1–3P2-B03_4, doi: 10.1299/jsmermd.2014._3P2-B03_1.
[25] H. Barazesh and M. A. Sharbafi, "A biarticular passive exosuit to support balance control can reduce metabolic cost of walking," *Bioinspiration Biomimetics*, vol. 15, no. 3, Mar. 2020, Art. no. 036009, doi: 10.1088/1748-3190/ab70ed.
[26] R. D. Crowninshield and R. A. Brand, "A physiologically based criterion of muscle force prediction in locomotion," *J. Biomech.*, vol. 14, no. 11, pp. 793–801, 1981, doi: 10.1016/0021-9290(81)90035-X.
[27] L. Zhou, S. Bai, M. R. Hansen, and J. Rasmussen, "Modeling of human arm energy expenditure for predicting energy optimal trajectories," *Model., Identificat. Control, Norwegian Res. Bull.*, vol. 32, no. 3, pp. 91–101, 2011, doi: 10.4173/mic.2011.3.1.
[28] A. Wolf and S. Wartzack, "Parametric movement synthesis: Towards virtual optimisation of man-machine interaction in engineering design," in *Proc. 15th Int. Design Conf.*, Dubrovnik, Croatia, 2018, pp. 941–952.
[29] Y. Uno, "Optimization models of human movements," *J. Robot. Soc. Jpn.*, vol. 32, no. 6, pp. 525–529, 2014, doi: 10.7210/jrsj.32.525.
[30] T. Flash and N. Hogan, "The coordination of arm movements: An experimentally confirmed mathematical model," *J. Neurosci.*, vol. 5, no. 7, pp. 1688–1703, Jul. 1985, doi: 10.1523/JNEUROSCI.05-07-01688.1985.
[31] S. Zhai, P. Milgram, and W. Buxton, "The influence of muscle groups on performance of multiple degree-of-freedom input," in *Proc. SIGCHI Conf. Hum. Factors Comput. Syst. Common Ground (CHI)*, Vancouver, BC, Canada, 1996, pp. 308–315.
[32] I. Poupyrev, S. Weghorst, and S. Fels, "Non-isomorphic 3D rotational techniques," in *Proc. SIGCHI Conf. Hum. Factors Comput. Syst. (CHI)*, The Hague, The Netherlands, 2000, pp. 540–547.
[33] J. S. Artal-Sevil and J. L. Montanes, "Development of a robotic arm and implementation of a control strategy for gesture recognition through leap motion device," in *Proc. Technol. Appl. Electron. Teach. (TAEE)*, Seville, Spain, Jun. 2016, pp. 1–9.
[34] A. M. Carlsson, "Assessment of chronic pain. I. Aspects of the reliability and validity of the visual analogue scale," *Pain*, vol. 16, no. 1, pp. 87–101, 1983, doi: 10.1016/0304-3959(83)90088-X.

HIROKI KATO received the B.E. degree in mechanical engineering from Osaka Prefecture University, Japan, in 2016, and the M.E. degree from the Department of Mechanical Engineering and Science, Graduate School of Engineering, Kyoto University, in 2019.

His research in Kyoto University is focused on an operating method using foot motion and human-powered vehicle.

Mr. Kato is a member of the Japan Society of Mechanical Engineers (JSME). He received the JSAE Graduate School Research Encouragement Award, in 2019.

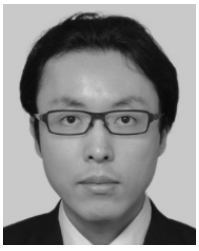

TATSURO TERAKAWA received the B.E. degree in mechanical engineering from Kyoto University, Japan, in 2014, and the M.E. and Dr.Eng. degrees from the Department of Mechanical Engineering and Science, Graduate School of Engineering, Kyoto University, in 2016 and 2019, respectively.

Since 2019, he has been an Assistant Professor with the Department of Mechanical Engineering and Science, Kyoto University. His research in Kyoto University is focused on mechanisms and control of wheeled mobile robots, actuator mechanisms, and design.

Dr. Terakawa is a member of JSME and the Japan Society of Design Engineering (JSDE). He received the JSME Miura Award in 2016, the JSME MD&T Division Encouragement Presentation in 2016, the JSME Medal for Outstanding Paper in 2018, the JSDE Encouragement Award in 2018, the IFToMM World Congress Best Application Paper Award in 2019, the FA Foundation Paper Award in 2019, the FFIT Research Encouragement Award in 2020, and the JSAE Graduate School Research Encouragement Awards in 2016 and 2019.

MASAHARU KOMORI (Member, IEEE) received the B.E. degree in precision engineering from Kyoto University, in 1995, the M.E. degree from the Graduate School, Kyoto University, in 1997, and the Ph.D. degree in engineering from Kyoto University, in 2002.

In 2000, he became a Research Assistant with the Graduate School of Engineering, Kyoto University. In 2004, he became an Associate Professor with Kyoto University. In 2017, he became a Professor with Kyoto University, where he belongs to the Department of Mechanical Engineering and Science. His research interests include riding robotics, vehicles, robots, operation, transmission, gear, and measurement.

Dr. Komori is a Fellow of JSME and a member of the Robotics Society of Japan (RSJ), JSDE, and the Japan Society for Precision Engineering (JSPE). He was a recipient of the JSME Young Engineers Award in 2005, the Young Scientists' Prize of The Commendation for Science and Technology by the Minister of Education, Culture, Sports, Science and Technology in 2011, the Best Paper Award from JSDE in 2012, the Eiji Mutoh Excellent Design Award in 2012, the Funai Academic Award (Funai Tetsuro Special Award) in 2012, the WT Award in 2013, three JSME Medals for Outstanding Paper in 2009, 2013, and 2018, the JSME Medal for New Technology in 2014, the Ichimura Prize in Science for Distinguished Achievement in 2014, two FA Foundation Paper Awards in 2014 and 2019, and the Nagamori Award in 2017. His paper was selected as one of the Best Articles published in Measurement Science and Technology, in 2009.

IKKO YASUDA received the B.E. degree in mechanical engineering from Kyoto University, Japan, in 2018, and the M.E. degree from the Department of Mechanical Engineering and Science, Graduate School of Engineering, Kyoto University, in 2020.

His research in Kyoto University is on an operating method using foot motion.